Chalcogenide Letters Vol. 17, No. 3, March 2020, p. 133 - 145

INDIUM INCORPORATION EFFECTS ON OPTICAL PROPERTIES OF QUATERNARY CHALCOGNIDE Se-Zn-Te-In FILMS

M. M. SORAYA[a], E. R. SHAABAN[b,*], M. I. EMAN[a], A. QASEM[c], S A. MAHMOUD[d], E. YOUSEF[e,f]

[a]*Department of Physics, Faculty of Science, Aswan University*

[b]*Physics Department, Faculty of Science, Al-Azhar University, Assuit, 71542, Egypt*

[c]*Physics Department, Faculty of Science, Al-Azhar University, Nasr City 11884, Cairo, Egypt*

[d]*Physics Department, Faculty of Science, Northern Border University, Arar 91431, Saudi Arabia.*

[e]*Physics Department, Faculty of Science, King Khalid University, P.O. Box 9004, Abha, Saudi Arabia*

[f]*Research Center for Advanced Materials Science (RCAMS), King Khalid University, Abha 61413, P.O. Box 9004, Saudi Arabia*

Amorphous semiconducting thin films of $Se_{90-x}Zn_5Te_5In_x$ (x=0, 2, 4, 6, 8 and 10 at. %) are deposited on glass substrates by thermal evaporating technique with thickness about of 1000 nm. The transmittance spectra are investigated by Swanepoel method to compute the optical coefficients and parameters in the spectral region of (400–2500) nm, such as absorption coefficient α, extinction coefficient k, optical band gap, E_g and refractive index, n. The optical absorption edge is described by using the non-direct transition model in terms of Tauc relation. The obtained values of both n and k were found to be dependent of the In content in the investigated samples. Also, other parameters have been computed like the real, (ε_r) and imaginary (ε_i) parts of complex dielectric constants. The dispersion parameters (dispersion energy, E_d, oscillation energy E_o) were discussed according to the single oscillator Wemple–DiDomenico model. The non-linear refractive index, n_2 was computed by using Tichy-Ticha and Fourier-Snitzer relationships.

(Received November 14, 2019; Accepted March 13, 2020)

Keywords: Chalcogenide glasses, Thin films, Optical parameters, Non-linear refractive index

1. Introduction

Chalcogenide glasses are one of unique groups of amorphous structures, due to their outstanding properties such as low phonon energy, high photosensitivity, high refractive index ($2.0 \geq n \geq 3.7$), high transparency in the infrared region and a high second/third-order optical nonlinearity [1–5]. Therefore, chalcogenide glasses have received great scientific and technical interests for many potential applications such as xerography switching, memory devices, photolithographic process, chemical sensing, scanning near field microscopy/spectroscopy, IR sources/lasers, realization of microstructures in integrated optics, fabrication of inexpensive solar cells, and more recently as reversible phase change optical recorders [1, 6–9].

Selenium-based chalcogenide glasses have advantages of high transparency in the broad middle and far IR regions in addition to strong nonlinear properties [10], low thermal conductivity, low melting point and exceptional stability, allowing for the formation of glasses while doping with various other elements [11,12]. Tellurium on the other hand supplies properties which are needed now days in cutting edge technologies based on chalcogenide glasses [13]. These properties mostly include transmittance in the far infra-red region which is used in optical fiber and IR optics [1, 14] and ultrafast crystallization which is used in phase change optical data storage devices [15–18]. Even though Se-based chalcogenide glasses have great applications,

*Corresponding author: esam_ramadan2008@yahoo.com

thermal instability leading to crystallization is considered as one of the draw backs of these alloys. Many researchers have tried to enhance the stability of Se–Te by addition of a third element. Addition of a third element to binary selenium alloy results remarkable change in the optical, electrical and thermal properties of chalcogenide glasses. In recent years, Zn containing ternary chalcogenide glasses attracted considerable interest since it has higher melting point, metallic nature, and advanced scientific interest [19].To enlarge applications of Se-Te-Zn films; Indium is added which has a large electro-negativity difference with Se and Te. The addition of In expands the glass forming area, creates compositional and configurationally disorder in the system and modify the structure, electrical and thermal properties of the ternary Se–Te-Zn system [20–25].

Among the interesting properties of chalcogenides glasses, optical properties have been the subject of intense studies to extract critical-material parameters, includes band structure, optical band gap, absorption coefficient, dispersion of refractive index. Knowledge of these parameters can develop their potential technological applications.

Chalcogenide thin films are experimentally prepared by different techniques includes thermal evaporation, chemical deposition, laser sputtering, and others [26, 27]. Preparations conditions, film thickness and deposition rate have vital effect on the optical features of the resultant thin films. In thin film terminology, thin film stack consists of thin absorbing layer (d_{film}= 600-1200 nm) of semiconducting material deposited on thick substrate (d_{Subs} =1-2 mm). Therefore, thin film stack is consisted of three successive interfaces, which are: air-film, film-substrate and substrate-air. Hence, multiple reflections and transmissions of the incident light waves at the film stack occur. However, if the optical thickness of the film is enough to generate several interference extremes, it is possible to calculate the optical constants such as the refractive index and extinction coefficient from only the transmittance data [28–33]. A simple and straightforward method has been proposed by Swanepoel based on the use of the extremes of the interference fringes of transmission spectrum alone for determining the optical constants [33].

The aim of this work, studied of the effect of In at expense of Se on the optical properties of $Se_{90-x}Te_5Zn_5In_x$ (x=0, 2, 4, 6, 8 and 10 at. %) thin films, based on a proposal from Swanepoel's to computed the optical parameters employ only the transmission spectra. The famous Swanepoel's method has been inserted to deduce the refractive index, film thickness, the extinction coefficient (k) and then the rest of the optical parameters and constants in the transparent region. The dispersion parameters are discussed using Single-oscillator Wemple-DiDomenico model. Also, Non-linear refractive index was calculated. All these parameters are very important for applications in optoelectronic devices.

2. Experimental details

Bulk chalcogenide samples of $Se_{90-x}Zn_5Te_5In_x$ (x = 0, 2, 4, 6, 8 and 10 at. %) were prepared based on the conventional melt-quenched technique. The high-purity elements were weighed and placed together in a preleased and outgassed silica ampoule, which was evacuated to a pressure of about 10^{-4} Pa and then sealed. The synthesis was performed in a rocking furnace at a temperature of approximately 950 ◦C, for about 24 h. After the synthesis, the melt was quenched in water at 273 K to obtain the Se-Zn-Te-In glassy alloy. The glass thin films were deposited onto well-cleaned glass substrates kept at room temperature by thermal evaporation technique using a coating unit (DV-502A; Denton Vacuum, Cherry Hill, NJ, USA) under high vacuum conditions (10^{-6} Pa). The deposition rate was adjusted to 10 Å/s which was continuously measured using a quartz crystal DTM 100 monitor. With this deposition rate, the chemical composition of the prepared films was found to be close to that of the starting bulk material. The thicknesses of the as-deposited films studied are about 1000 nm to avoid the effect of film thickness. During the deposition process, the substrates were kept at room temperature 300 K. The substrates were rotated at slow speed 5 Rev/min to obtain a homogenous and smooth film. In evaporation process, FTM6 thickness monitor is used to display the thickness of the produced films. X-ray diffraction (XRD) Philips diffractometry (1710), with Cu-K_{a1} radiation (λ=1.54056 Å) have been used to confirm the amorphous nature of the deposited films. The optical transmittance T and reflectance R of the deposited films were measured using a UV–Vis–NIR JASCO-670 double-beam

spectrophotometer. The transmittance spectra in the wave length range (400–2500 nm) were collected at normal incidence without a substrate in the reference beam, whereas the reflectance spectra were measured using a reflection attachment closes to normal incidence (~5°). All the optical measurements were made at room temperature.

3. Results and discussion

3.1. Structural properties

XRD analysis results of the as-deposited films grown on silica glass substrate are represented in Fig. 1. The XRD patterns demonstrate that the films exhibit mainly amorphous structure and do not exhibit any sharp peaks for crystalline phase. The X-ray intensity data were collected in the angular ranges 2θ = 5-90°. The presence of two amorphous humps may be clarified in terms of the finding of two amorphous phases of glass.

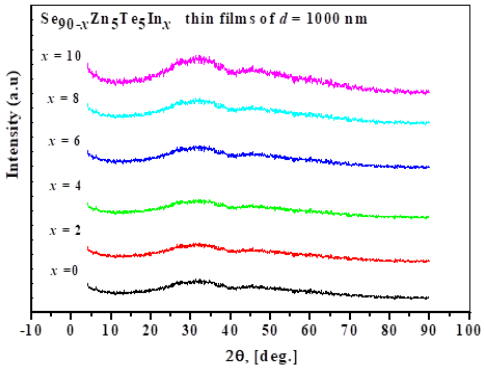

Fig. 1. X-ray diffraction patterns of $Se_{90-x}Zn_5Te_5In_x$ ($0 \le x \le 10$) thin films.

3.2. Effect of In additive on the optical properties of Se-Te-Zn thin films

The spectral dependence of the optical transmittance, *T* and the reflectance, *R* of the investigated samples can be obtained. Fig. 2 shows the transmittance, *T* and reflectance, *R* spectra of the deposited films as a function of wavelength. The 'non-shrinking' interference fringes (fringes of equal chromatic order, FECO) observed in the transmittance spectra at wavelength (800-2000nm) indicates the homogeneity and smoothness of the deposited films. Moreover, the absorption edge moves towards the less photon energy as In contents increases in the Se-Zn-Te glass. This could be attributed to decreasing the energy gap as a result of In substitution for Se atoms in the mentioned Se-Zn-Te glass.

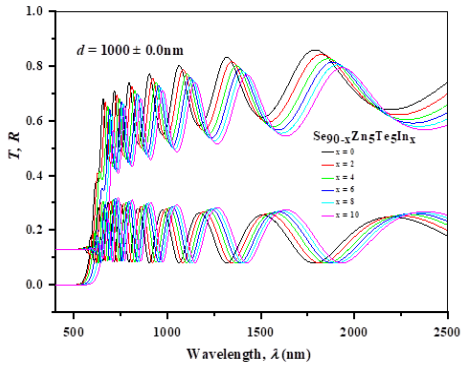

Fig. 2. A typical optical transmission–reflection spectra of amorphous $Se_{90-x}Zn_5Te_5In_x$ ($0 \le x \le 10$) thin films.

According to Swanepoel's method, which is based on the idea of creating upper and lower envelopes of the transmittance spectrum [34]. It showed the construction of the two envelopes T_M (λ) and T_m (λ) in all studied samples. The values of T_M (λ) and T_m (λ) for (the sample: 1) are illustrated in Fig. 3 and listed in Tables 1. We considered (the sample: 1) as a mathematical example for other samples that were calculated in the same way.

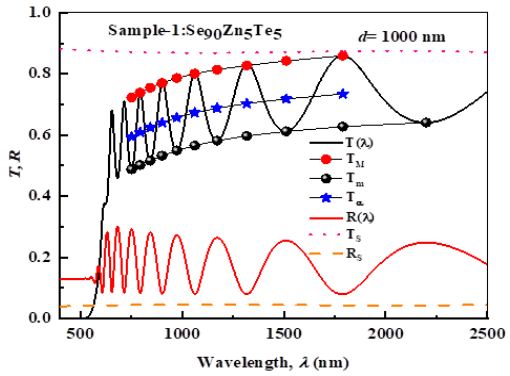

Fig. 3. A typical optical transmission-reflection spectrum of $Se_{90}Zn_5Te_5$ thin film. The T_{max} and T_{min} are shown as red and black circle, respectively.

3.3. Determination of the refractive index and the film thickness

The refractive index n is a significant parameter, which is an essential property for the practical applications. It is associated with the electronic polarizability of ions as well as electric field within the material. Both the refractive index n and the film thickness of $Se_{90-x}Zn_5Te_5In_x$ thin films can be computed as follows:

The necessary values of the refractive index of the substrate, s, are obtained from the transmission spectrum of the substrate, T_s, by using the well-known equation [35]

$$s = \frac{1}{T_s} + \left(\frac{1}{T_s} - 1\right)^{\frac{1}{2}} \tag{1}$$

Based on Manifacier *et al* idea [34] of creating the upper and lower envelopes Fig. 3 of interference fringes, Swanepoel have introduced a method for analyzing a first, approximate value of the refractive index of the film n_1, in the spectral region of medium and weak absorption, according to the expression

$$n_1 = \left[N_1 + \left(N_1^{\,2} - s^2\right)^{1/2}\right]^{1/2} \tag{2}$$

where

$$N = 2s\frac{T_M - T_m}{T_M T_m} + \frac{s^2 + 1}{2} \tag{3}$$

Here T_M and T_m, are the transmission maximum and the corresponding minimum at a certain wavelength λ. Alternatively, one of these values is an experimental interference extreme and the other one is derived from the corresponding envelope; both envelopes were computer generated using the origin version 7 program using more than one procedure. The values of the refractive index n_1, as computed from Eq. (2), are shown in Table 1.

Table 1. Values of two envelopes T_M and T_m of (the sample: 1). The computed values of refractive index and film thicknesses are based on the envelope method.

x at.%	λ_e(nm)	T_M	T_m	S	n_1	d_1 (nm)	m_o	m	d_2(nm)	n_2
	752	0.7227	0.4879	1.419	2.54	--	7.07	--	--	2.56
	794	0.7385	0.5019	1.422	2.51	1106.40	6.62	6.5	1025.27	2.51
	844	0.7548	0.516	1.425	2.48	1063.92	6.16	6	1017.05	2.46
	902	0.7705	0.5326	1.427	2.45	1049.64	5.67	5.5	1011.78	2.42
	974	0.786	0.5492	1.430	2.41	1044.07	5.18	5	1008.17	2.37
***x*=0**	1062	0.8008	0.5655	1.432	2.38	1024.59	4.68	4.5	1003.74	2.33
	1172	0.814	0.5815	1.433	2.34	1016.87	4.17	4	999.57	2.29
	1318	0.8274	0.5971	1.433	2.31	1005.72	3.66	3.5	997.93	2.25
	1512	0.8427	0.6120	1.429	2.28	--	3.15	3	993.93	2.22
	1790	0.8594	0.6275	1.419	2.24	--	2.62	2.5	994.85	2.18
	$\overline{d_1} = 1044.46$ nm $\sigma_1 = 31.39$ (3 %)					$\overline{d_2} = 1005.81$ nm $\sigma_2 = 10.07$ (1%)				

If n_{e1} and n_{e2} are the refractive indices at two adjacent maxima (or minima) at λ_1 and λ_2, it follows that the film thickness is given by the expression:

$$d = \frac{\lambda_1 \lambda_2}{2\left(\lambda_1 n_{e2} - \lambda_2 n_{e1}\right)} \tag{4}$$

The values of film thickness are listed in Table 1 as d_1. Also, the average value of d_1, corresponding to the (sample: 1) is listed in Table 1.

It is necessary to consider the basic equation for interference fringes:

$$2nd = m\lambda \tag{5}$$

where the order number m is an integer for maxima and a half integer for minima, this value of m can now be used, along with n_1, to calculate the 'order number' m_0 for the different extremes using Eq. (5).

The accuracy of d can now be significantly increased by taking the corresponding exact integer or half integer values of m associated with each extreme Fig. 3 and deriving a new thickness, d_2 from Eq. (5), again using the values of n_1, the values of d_2 found in this way have a smaller dispersion ($\sigma_1 > \sigma_2$). It should be highlighted that the accuracy of the final thickness is approximately better than 1% (Table 1).

The accurate value of n in Eq. (5) can be solved by the exact value of m at each λ and, thus, the final values of the refractive index n_2 are obtained as listed in Table 1.

Now, the dependence of n on wavelength of the studied thin films is showed in Fig. 4. The values of the refractive index increase with the increase in the concentration of the In content. This increase is related to the increased polarizability of the larger In atomic radius 2.00 Å compared with the Se atomic radius 1.22 Å. To induce the refractive index in both strong absorption region

and transparent region, the Cauchy equation is used which is valid in thin film model. Now, the values of *n* can be fitted to a reasonable dispersion function such as the two-term Cauchy function, $n(\lambda) = a + b/\lambda^2$, which can be used for extrapolation the whole wavelength dependence of refractive index Fig. 4. The values of Cauchy coefficient, *a* and *b* are listed in Table 2.

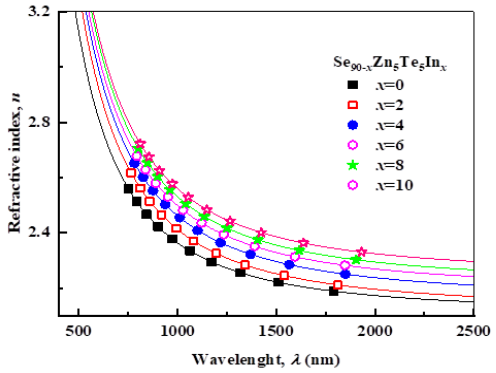

Fig. 4. Dispersion of refractive index, n versus wavelength, λ of amorphous $Se_{90-x}Zn_5Te_5In_x$ ($0 \le x \le 10$) thin films.

Table 2. The values of fitted Cauchy coefficients (a and b) of amorphous $Se_{90-x}Zn_5Te_5In_x$ thin films.

Refractive index, $n = a + \frac{b}{\lambda^2}$		***x* at. %**
b $(nm)^2$	a	
254833.2	2.109	**0**
289144.1	2.123	**2**
299321.2	2.163	**4**
305886.9	2.193	**6**
315103.5	2.215	**8**
314045.9	2.246	**10**

3.4. Determination of the optical parameters

In the strong absorption region, the absorption coefficient α can be obtained of the experimentally measured values of *R and T* according to the following expression [36]:

$$\alpha = \frac{1}{d} \ln \left[\frac{(1-R)^2 + \left[(1-R)^4 + 4R^2T^2 \right]^{1/2}}{2T} \right] \quad (6)$$

where *d* is the sample thickness. Fig. 5 shows the absorption coefficient as a function of photon energy for the different compositions. It is clear that with increasing In contents in all the specimens under study, the absorption edge ($\alpha \ge 10^4$) shifts towards the less photon energy that is related to the decreasing of the optical band gap with the variation of the different chemical compositions as a result of In additive.

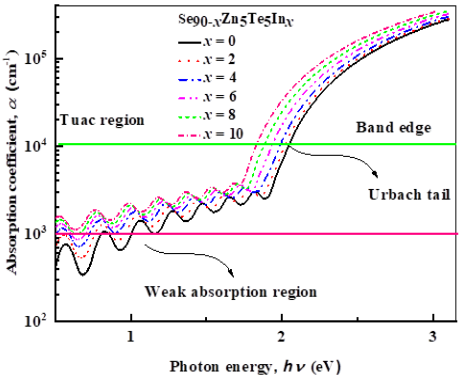

Fig. 5. The absorption coefficient, α versus photon energy, hν of amorphous $Se_{90-x}Zn_5Te_5In_x$ ($0 \le x \le 10$) thin films.

The extinction coefficient can now be obtained from the values of λ and α using the formula, $k = [\alpha\lambda/4\pi]$. The dependence of k on the wavelength of the studied thin films is illustrated in Fig. 6. The extinction coefficient decreases with an increase in wavelength due to low loss of the fraction of light because of scattering and absorbance process. It is seen that the extinction coefficient is increasing with an increase in In content for entire wavelength (400-750 nm). The increase in number of localized states result in more scattering losses and increase in the k value.

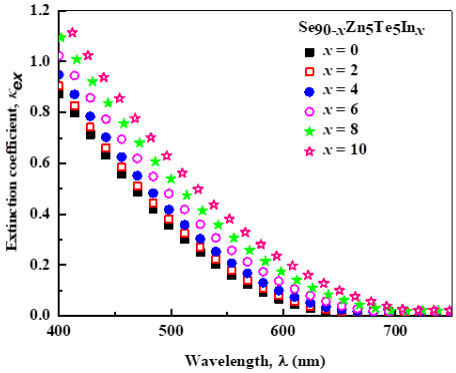

Fig. 6. The extinction coefficient, k versus wavelength, λ of amorphous $Se_{90-x}Zn_5Te_5In_x$ ($0 \le x \le 10$) thin films.

The absorption coefficient of amorphous semiconductors, in the high-absorption region ($\alpha \ge 10^4$), is given according to Tauc's relation for the allowed non-direct transition [37] by the following equation:

$$\alpha(h\nu) = \frac{A(h\nu - E_g^{opt})^2}{h\nu} \tag{7}$$

where A is a constant which depends on the transition probability and E_g^{opt} is the optical band gap. Fig. 7 shows $(\alpha h\nu)^{1/2}$ versus photon energy ($h\nu$) for the six different composition thin films. The values of the optical band gap E_g^{opt} were taken as the intercept of $(\alpha h\nu)^{1/2}$ versus ($h\nu$) at $(\alpha h\nu)^{1/2} = 0$ according to Tauc's relation for the allowed non-direct transition.

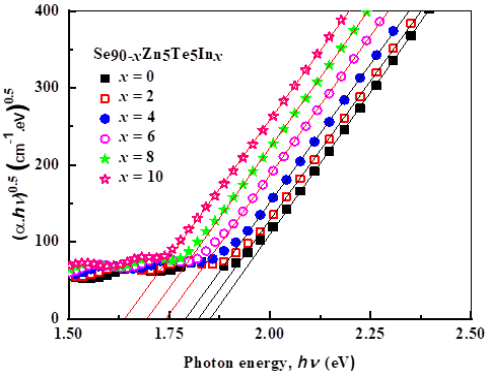

Fig. 7. The dependence of $(\alpha h\nu)^{1/2}$ on photon energy, hν of amorphous $Se_{90-x}Zn_5Te_5In_x$ $(0 \le x \le 10)$ thin films.

Table 3. Values of energy gap, E_g^{opt}, width of localized states, E_e, the single oscillator energy, E_o, the dispersion energy, E_d and the static linear refractive index, n_o, of amorphous $Se_{90-x}Zn_5Te_5In_x$ thin films.

Dispersion parameters				**Optical parameters**	
x	E_o **(eV)**	E_d **(eV)**	$n(o)$	E_g^{opt} **[indir] (eV)**	E_e **(eV)**
0	3.389	14.59	2.30	1.85	0.168
2	3.296	14.91	2.35	1.82	0.173
4	3.276	15.47	2.39	1.79	0.176
6	3.262	15.88	2.42	1.74	0.179
8	3.250	16.30	2.45	1.69	0.184
10	3.247	16.59	2.47	1.63	0.189

The optical band gap derived for each film is listed in Table 3. According to Urbach relation [38], the absorption depends exponentially on the photon energy at lower values of the absorption coefficient ($1 \le \alpha \le 10^4$ cm^{-1}):

$$\alpha(h\nu) = \alpha_0 \exp\left(\frac{h\nu}{E_e}\right) \tag{8}$$

where α_0 is a constant and E_e is the Urbach energy (related to the width of the band tail of the localized states at the conduction or valence band edge). Fig. 8 shows the dependence of ln(α) on photon energy $h\nu$ of the studied thin films, from which the Urbach energy E_e is estimated. The values of E_e (the Urbach energy) are computed and listed in Table 3. It is obvious that Energy gap, E_g^{opt} decreases with increasing In content but the Urbach energy E_e increases, this mean that an additional of In lead to an increase of the localized states within the band gap. Davis and Mott [39] informed that the presence of high density of localized state in the band structure is responsible for

the lower values of optical gap. It seems that our results have a good agreement with Davis and Mott suggestion.

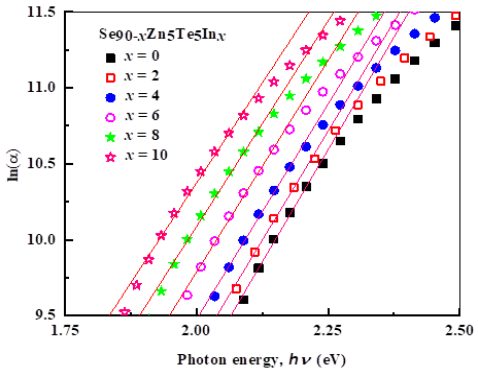

Fig. 8. The dependence of ln(α) on photon energy, hν of amorphous $Se_{90-x}Zn_5Te_5In_x$ ($0 \le x \le 10$) thin films.

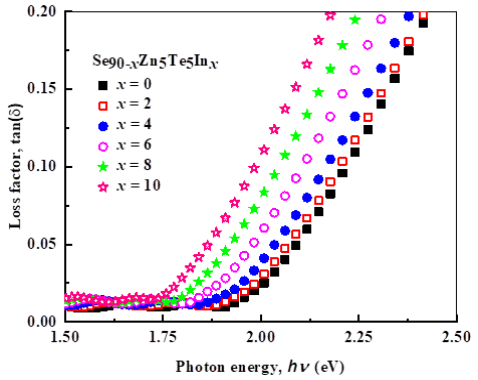

Fig. 9. The variations of loss factor as a function of photon energy, hν of amorphous $Se_{90-x}Zn_5Te_5In_x$ ($0 \le x \le 10$) thin films.

3.5. Determination of the loss factor

Dielectric properties have significant role in electrical applications thus; studying and determining ε has some extent of importance. It has two parts; the real, ε_r and imaginary parts, ε_i. These of parameters are functions in *n* and *k* and can be computed based on [40]:

$$\varepsilon = \varepsilon_r + i\,\varepsilon_i \tag{9}$$

$$\varepsilon_r = n^2 - k^2 \tag{10}$$

$$\varepsilon_i = 2nk \tag{11}$$

Loss factor (dissipation factor) can be deduced of the ratio of the imaginary part to the real part of the dielectric constant [41]:

$$\tan(\delta) = \frac{\varepsilon_i}{\varepsilon_r} \tag{12}$$

The variations of loss factor as a function of photon energy is plotted in Fig. 9. With increasing photon energy, loss factor increases.

3. 6. Determination of the dispersion parameters

The refractive index dispersion has been investigated by using Wemple and DiDomenico (WDD) single oscillator model [42, 43], where the optical data could be described to an excellent approximation by the following expression:

$$(n^2-1)^{-1} = \frac{E_o}{E_d} - \frac{1}{E_o E_d}(h\nu)^2 \tag{13}$$

where h is Planck's constant, ν is the frequency, $h\nu$ is the photon energy, E_o is the single-oscillator energy and E_d is the dispersion energy. The physical meaning of E_d is related to the average strength of inter-band optical transitions and is associated with the changes in the structural order of the material and the effective oscillator energy, while E_o can directly correlate with the optical energy gap by an empirical formula ($E_o \approx 2E_g$) [44]. E_o is considered as an average band gap, the so-called WDD band gap, and it corresponds to the distance between the 'centers of gravity' of the valence and the conduction bands: E_o is, therefore, related to the bond energy of the different chemical bonds present in the material. Plotting $(n^2-1)^{-1}$ versus $(h\nu)^2$ and filling the data to a straight line Fig. 10.

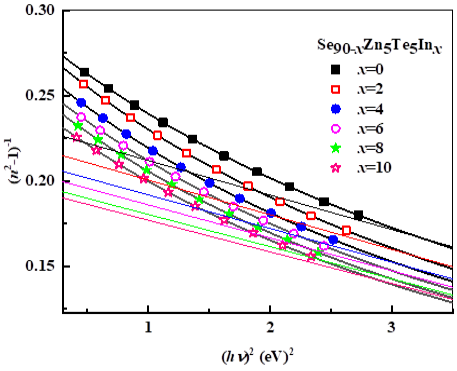

Fig. 10. Plot of refractive index factor $(n^2-1)^{-1}$ versus $(h\nu)^2$ of amorphous $Se_{90-x}Zn_5Te_5In_x$ $(0 \le x \le 10)$ thin films.

E_o and E_d can be determined from the intercept, E_o/E_d and the slope, $(-1/E_o E_d)$. The static refractive index n_o (at zero photon energy) is calculated by extrapolating the WDD dispersion equation to $h\nu \rightarrow 0$ (the static refractive index), gives the equation:

$$n_o = [1 + \frac{E_d}{E_o}]^{\frac{1}{2}} \tag{14}$$

The obtained values of E_o, E_d and n_o for the studied thin films are listed in Table 3. It was observed that, with increasing In content, the single-oscillator energy E_o decreases while the dispersion energy E_d and the static refractive index, n_o increases. E_d increases with increasing In content, while there is a decrease in the Se-Se homopolar bonds. It means indium is more coordinated in the glass matrix. The value of E_d increases with increasing In content, due to the increase in the effective coordination of the cation.

3.7. Determination of the non-linear refractive index

In terms of Tichy and Ticha relationship [45], The nonlinear refractive index, n_2 was deduced. Tichy and Ticha relationship is a combination of Miller's popularized rule and static refractive index computed from WDD model as [45, 46]:

$$n_2 = [\frac{12\pi}{n_o}]\chi^{(3)} \tag{15}$$

where $\chi^{(3)}$ is third order non-linear susceptibility and computed from the following relation [47]:

$$\chi^{(3)} = A[\chi^{(1)}]^4 \tag{16}$$

where $\chi^{(1)}$ is linear susceptibility which is expressed as:

$$\chi^{(1)} = \frac{1}{4\pi}[\frac{E_d}{E_o}] \tag{17}$$

where $A = 1.7\times10^{-10}$ (for $\chi^{(3)}$ in *esu*). Therefore, $\chi^{(3)}$ is expressed as:

$$\chi^{(3)} = \frac{A}{(4\pi)^4}\left(n_o^2 - 1\right)^4 \tag{18}$$

Fig. 11 plots the non-linear refractive index according to Tichy and Ticha relationship versus wavelength of the investigated samples. The non-linear refractive index decreases with increasing wave length and increases with increasing In content.

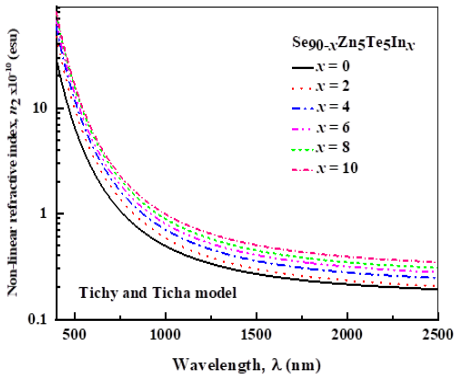

Fig. 11. Plots the non-linear refractive index according to Tichy and Ticha relationship versus wavelength of the studied samples.

Fournier and Snitzer [48] proposed another way to computed the non-linear refractive index on the basis of linear refractive index (n) and WDD parameters (E_o, E_d) in the following relation:

$$n_2 = \frac{(n^2+2)^2(n^2-1)}{48\pi nN}[\frac{E_d}{E_o^2}] \tag{19}$$

where N is the density of polarizable constituents which is computed by using density/molar volume data. The nonlinear refractive index is deduced in *esu* [49, 50].

Fig. 12 shows the variation in nonlinear refractive index, n_2 according to Fournier and Snitzer relationship with wavelength. Also, the values of non-linear refractive index n_2 do the same

as with Tichy and Ticha, i.e. decrease with increasing wave length and increase with increasing In content.

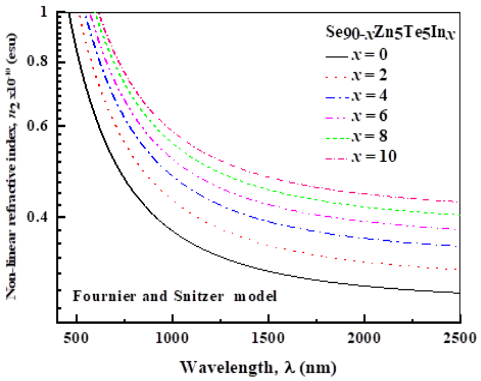

Fig. 12. Plots the variation in nonlinear refractive index, n_2 according to Fournier and Snitzer relationship with wavelength of the studied samples.

4. Conclusion

XRD patterns of thermally evaporated films of $Se_{90-x}Zn_5Te_5In_x$ (x=0, 2, 4, 6, 8 and10 at. %) alloys ensure the amorphous nature for all the samples. Analyzing the results of the optical measurements showed that:

- The optical band gap of the studied films decreases slightly with increasing In content, the value of E_g decreases from 1.85 to 1.63 eV. This decrease may be correlated with the increase of the localized states within the band gap by the additional of In.
- The values of the refractive index increase with the increase in the concentration of the In content. This result is related to the increased polarizability of the larger In atomic radius 2.00 Å compared with the Se atomic radius 1.22Å.
- The extinction coefficient has the same behavior of refractive index; reduce for all the investigated films with increasing the wavelength of incident photons, increasing with increasing In content.
- The dispersion parameters such as E_d, n_o increase with increasing In content while E_o decreases.
- Non-linear refractive index, n_2 was estimated according to two models Tichy-Ticha and Fourier-Snitzer. The two models ensure that the non-linear refractive index decreases with increasing wave length and increases with increasing In content.

Acknowledgments

The authors are grateful to the Deanship of Scientific Research at King Khalid University (KKU) for funding this research project, Number: (R.G.P2./62/40) under research center for advanced material science

References

[1] A. Zakery, S. R. Elliott, Journal of Non-Crystalline Solids **330**(1-3), 1 (2003).
[2] Sanghera, Jas, and Ishwar D. Aggarwal. Infrared fiber optics. CRC Press, 1998.
[3] V. Ilcheva et al., Physics Procedia **44**, 67 (2013).
[4] Ishwar D. Aggarwal, Jas S. Sanghera, J. Optoelectron. Adv. Mater **4**(3), 665 (2002).
[5] Qiming Liu et al., Optics letters **26**(17), 1347 (2001).

[6] Stanford R. Ovshinsky, Physical Review Letters **21**(20), 1450 (1968).
[7] N. F. Mott, Philosophical Magazine **24**(190), 935 (1971).
[8] David E. Carlson, Cristopher R. Wronski, Applied Physics Letters **28**(11), 671 (1976).
[9] Fusong Jiang, Masahiro Okuda, Japanese journal of applied physics **30**(1R), 97 (1991).
[10] Shuo Cui et al., Molecules **18**(5), 5373 (2013).
[11] Y. Sung-Min et al, IEEE Electron Device Lett. **27**, 445 (2006).
[12] Yegang Lu et al., ECS Solid State Letters **2**(10), P94 (2013).
[13] Roman Svoboda, Miloslav Kincl, Jiří Málek, Journal of Alloys and Compounds **644**, 40 (2015).
[14] Allison A. Wilhelm et al., Advanced Materials **19**(22), 3796 (2007).
[15] Simone Raoux, Wojciech Wełnic, Daniele Ielmini, Chemical reviews **110**(1), 240 (2009).
[16] M. Wuttig, C. Steimer, Applied Physics A **87**(3), 411 (2007).
[17] M. Wuttig, N. Yamada, Phase-change materials for rewriteable data storage, Nat. Mater. **6**, 824 (2007).
[18] Wojciech Wełnic et al., Journal of Materials Research **22**(9), 2368 (2007).
[19] M. M. Soraya et al., Applied Physics A **124**(2), 197 (2018).
[20] E. R. Shaaban et al., Applied Physics A **122**(1), 20 (2016).
[21] N. Goyal, Abdolali Zolanvari, S. K. Tripathi, Journal of Materials Science: Materials in Electronics **12**(9), 523 (2001).
[22] Arvind Kumar et al., X‐Ray Spectrometry **19**(5), 243 (1990).
[23] R. M. Mehra, A. Ganjoo Gurinder, P. C. Mathur, Journal of thermal analysis **45**(3), 405 (1995).
[24] A. B. Gadkari, J. K. Zope, Journal of non-crystalline solids **103**(2-3), 295 (1988).
[25] Shaaban, E. R., Kansal, I., Mohamed, S., Ferreira, Physica B: Condensed Matter. 404 (2009) 3571.
[26] M. M. El-Samanoudy, Thin Solid Films **423**(2), 201 (2003).
[27] S. Venkatachalam, D. Mangalaraj, Sa K. Narayandass, Journal of Physics D: Applied Physics **39**(22), 4777 (2006).
[28] E. Márquez et al., Optical Materials **2**(3), 143 (1993).
[29] E. R. Shaaban et al., Physica B: Condensed Matter **381**(1-2), 24 (2006).
[30] V. Ilcheva et al., Applied Surface Science **255**(24), 9691 (2009).
[31] Z. Cimpl, F. Kosek, Physica status solidi A **93**(1), K55 (1986).
[32] R. Swanepoel, Journal of Physics E: Scientific Instruments **17**(10), 896 (1984).
[33] E. R. Shaaban, Philosophical Magazine **88**(5), 781 (2008).
[34] J. C. Manifacier, J. Gasiot, J. P. Fillard, Journal of Physics E: Scientific Instruments **9**(11), 1002 (1976).
[35] F. A. Jenkins, H. E. White, Fundamentals of Optics, McGrow-Hill, New York, 1957.
[36] R. Valalova, L. Tichy, M. Vlcek, H. Ticha Phys. Status Solidi A **181**, 199 (2000).
[37] J. Tauc, Amorphous and Liquid Semiconductors. Springer, Boston, MA, 159 (1974).
[38] Franz Urbach, Physical Review **92**(5), 1324 (1953).
[39] E. A. Davis, N. F. F. Mott, Philosophical Magazine **22**(179), 0903 (1970).
[40] A. El-Denglawey, M. M. Makhlouf, M. Dongol, Results in Physics **10**, 714 (2018).
[41] Amin El-Adawy, N. El Koshkhany, E. R. Shaaban, Journal of Physics and Chemistry of Solids **67**(8), 1649 (2006:.
[42] S. H. Wemple, M. DiDomenico Jr., Physical Review B **3**(4), 1338 (1971).
[43] S. H. Wemple, Physical Review B **7**(8), 3767 (1973).
[44] Keiji Tanaka, Thin solid films **66**(3), 271 (1980).
[45] H. Ticha, L. Tichy, J. Optoelectron. Adv. Mater. **4**(2), 381 (2002).
[46] R. Shaaban, Essam et al., Journal of the American Ceramic Society **102**(7), 4067 (2019).
[47] Charles C. Wang, Physical Review B **2**(6), 2045 (1970).
[48] J. Fournier, E. Snitzer, IEEE Journal of Quantum Electronics **10**(5), 473 (1974).
[49] Masaki Asobe, Terutoshi Kanamori, Ken'ichi Kubodera, IEEE journal of quantum electronics **29**(8), 2325 (1993:.
[50] T. Töpfer et al., Applied Physics B **71**(2), 203 (2000).